INSTITUTE OF PHYSICS PUBLISHING JOURNAL OF MICROMECHANICS AND MICROENGINEERING

J. Micromech. Microeng. **14** (2004) 604–611 PII: S0960-1317(04)71038-4

Nonlinear diffusive mixing in microchannels: theory and experiments

Zhigang Wu, Nam-Trung Nguyen and Xiaoyang Huang

School of Mechanical and Production Engineering, Nanyang Technological University, 50 Nanyang Avenue, 639798, Singapore

E-mail: mntnguyen@ntu.edu.sg

Received 27 October 2003
Published 6 February 2004
Online at stacks.iop.org/JMM/14/604 (DOI: 10.1088/0960-1317/14/4/022)

Abstract

Effective mixing is an important task in microfluidics for chemical and biochemical applications. Due to the small size and consequently the low Reynolds number, mixing in microchannels relies on diffusive transport. This paper discusses an analytical model of diffusive mixing in microchannels. The dimensionless analysis generalizes the solution for different channel sizes and different diffusion coefficients. The Peclet number is the only parameter of the model. Furthermore, the paper presents the result of a nonlinear model of diffusive mixing in microchannels. The nonlinear model considers the dependence of the diffusion coefficient on the concentration. A simple micromixer was fabricated using a lamination technique. Measurement results with the micromixer verify the analytical results.

(Some figures in this article are in colour only in the electronic version)

1. Introduction

Micromixers are indispensable components of microfluidic systems for chemical and biochemical applications. These systems are also called labs on a chip (LOC). In a LOC, a sample solution is often to be tested with a reagent. Effective mixing makes a complete reaction possible. A number of micromixers have been fabricated and tested in the past. Based on the mixing concept, micromixers can be categorized as passive micromixers and active micromixers [1].

Passive micromixers rely entirely on diffusion. Based on their configuration, passive mixers can be further categorized as lamination micromixers and injection micromixers. In lamination mixers, the fluid streams are split into several small streams, which are later joined in a mixing channel [2, 3]. The fluid streams can also be sequentially laminated and split for minimizing diffusion length [4, 5]. In contrast to lamination mixers, an injection mixer splits only one stream into many substreams in the form of microplumes, which increase the contact surface and decrease the mixing path [6].

Active micromixers use external fields to agitate the fluid. The agitating field can be pressure driven [7], acoustic [8], magneto hydrodynamic [9] or electrokinetic [10].

One of the simple passive micromixers is the Y-mixer. This mixer has two inlets and a single mixing channel. This mixer type was investigated numerically with a simplified two-dimensional model that neglects the diffusion in the flow direction [11]. A numerical model does not give enough insight into the mixing effects of this simple but important mixer type. Beard [12] introduced an effective dispersion coefficient for a two-dimensional model and an analytical solution including the diffusion in the flow direction. However, this model assumed zero flux of the diffusion in a finite small length, which is not always valid. Furthermore, the analytical solution in [12] is complex and difficult for further analysis. The solution for the same model was given in [13], where the diffusive effect in the flow direction was also neglected. All published models do not consider the nonlinear effect of the diffusion coefficient.

This paper presents a complete two-dimensional diffusive mixing model. The velocity field is assumed to be homogenous across the channel width. This situation appears in a Hele–Shaw flow or in an electronically driven flow. The model is solved and analyzed in a dimensionless manner, so that the only parameter for optimization is the Peclet number. Both linear and nonlinear models with a diffusion coefficient as a function of the concentration are discussed. The nonlinear model is important for designing fixed concentration arrays in microfludic devices. To the best knowledge of the authors,

 © 2004 IOP Publishing Ltd Printed in the UK

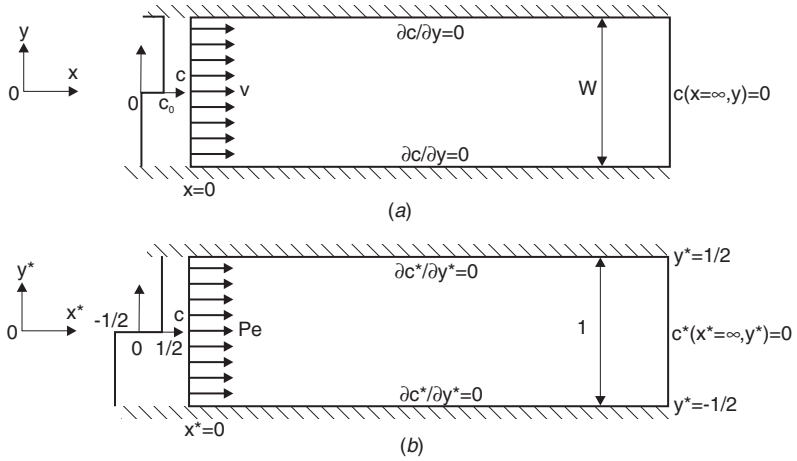

Figure 1. Two-dimensional model of a micromixer: (*a*) the actual model and (*b*) the dimensionless model.

all published fixed concentration arrays are based on the linear mixing model [13, 14]. A micromixer was fabricated and characterized for verifying the theoretical results. Results of this paper represent an analytical tool for parametric optimization of passive micromixers.

2. Analytical model of the micromixer

2.1. Linear model

In most macro-scale problems, the diffusion coefficient of a fluid pair is assumed to be constant. The diffusion coefficient D is defined by the Fick's law:

$$\Phi = -D\frac{\mathrm{d}c}{\mathrm{d}x}, \tag{1}$$

where Φ is the species flux and c is the concentration. The following analytical model assumes a constant diffusion coefficient D for the entire concentration range.

The two-dimensional model of a micromixer with two inlet streams is depicted in figure 1. The mixer is a long channel with a width of W, with two inlet streams. One stream is the solute with a concentration of c_0, the other stream is the solvent with a concentration of $c = 0$. The flow in the channel is assumed to have a constant velocity of u. The boundary conditions are depicted in figure 1(*a*). The transport equation for both diffusive and convective effects can be formulated as [16]

$$D\left(\frac{\partial^2 c}{\partial x^2} + \frac{\partial^2 c}{\partial y^2}\right) = u\frac{\partial c}{\partial x} \tag{2}$$

where D is the diffusion coefficient of the species. By introducing the dimensionless variables for the coordinate system $x^* = x/W$, $y^* = y/W$, the dimensionless concentration $c^* = c/c_0 - 1/2$ and the Peclet number:

$$Pe = \frac{uW}{D} \tag{3}$$

equation (2) can be formulated in the dimensionless form as

$$\left(\frac{\partial^2 c^*}{\partial x^{*2}} + \frac{\partial^2 c^*}{\partial y^{*2}}\right) = Pe\frac{\partial c^*}{\partial x^*}. \tag{4}$$

The model of (4) is depicted in figure 1(*b*). The boundary conditions for (4) are

$$\begin{aligned} c^*|_{(x^*=0,\,0<y^*<1/2)} &= 1/2 \\ c^*|_{(x^*=0,\,-1/2<y^*<0)} &= -1/2 \\ c^*|_{(x^*=\infty)} &= 0. \end{aligned} \tag{5}$$

The channel wall is impermeable. Thus, the boundary condition for the zero flux at the channel walls is

$$\left.\frac{\partial c^*}{\partial y^*}\right|_{y=\pm 1/2} = 0. \tag{6}$$

Separating the variables in (4) and applying the boundary conditions (5) and (6) results in the dimensionless concentration:

$$c^*(x^*, y^*) = \frac{1}{\pi}\sum_{n=1}^{\infty}\exp\left[\frac{Pe - \sqrt{Pe^2 + 4(2n-1)^2\pi^2}}{2}x^*\right] \times \sin[\pi(2n-1)y^*]\frac{1-\cos[\pi(2n-1)]}{2n-1}. \tag{7}$$

For large Peclet numbers, the diffusive term in the x^*-direction is much smaller than the convective term in (4). Thus, equation (4) can be simplified as

$$\frac{\partial^2 c^*}{\partial y^{*2}} = Pe\frac{\partial c^*}{\partial x^*}. \tag{8}$$

The solution of (8) with the same boundary conditions of (5) and (6) is

$$c^*(x^*, y^*) = \frac{1}{\pi}\sum_{n=1}^{\infty}\exp\left[\frac{-\pi^2(2n-1)^2x^*}{Pe}\right] \times \sin[\pi(2n-1)y^*]\frac{1-\cos[\pi(2n-1)]}{2n-1}. \tag{9}$$

A similar result was also derived in [13]. It is apparent that a short mixing length requires a small Peclet number, which corresponds to a slow velocity u, a small channel width W or a large diffusion coefficient D. For a typical aqueous solution with a diffusion coefficient on the order of 10^{-9} m^2 s^{-1}, flow velocity of 100 μm s^{-1} and a channel width of 100 μm the Peclet number is on the order of $Pe = 10$ and the liquids are fully mixed at $x^* \approx 2$.

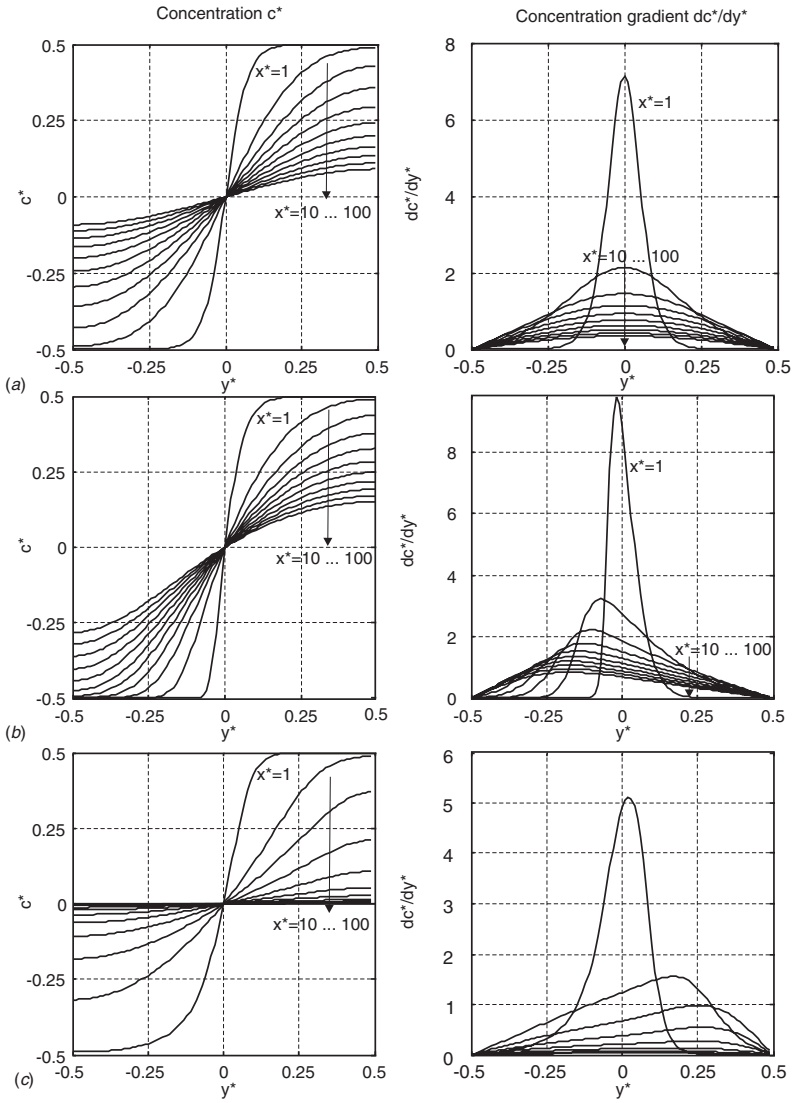

Figure 2. Distributions of concentration and concentration gradient across a microchannel ($Pe_0 = 50$): (*a*) ideal linear model $a = 1$, (*b*) nonlinear model, stronger interaction between solvent and solute $a = 0.2$ and (*c*) nonlinear model, weaker interaction between solvent and solute $a = 5$.

2.2. Nonlinear model

In microfluidic applications, due to the small channel size, concentration gradients are much higher than those in macroscale. The dependence of the diffusion coefficient on the concentration may have a bigger impact in microscale. A binary mixture of two species A and B is considered as ideal if the interactions between the pairs A–A, B–B and A–B are equal. However, in a real mixture the strength of the interactions differs from pair to pair depending on the concentration of each species [15]. Thus, the diffusion coefficient of a species depends on its own concentration.

We consider a simple model of a binary mixture between A and B, where A is the solute and B is the solvent. The diffusion coefficient of A at the maximum concentration $c = c_0$ is D_0. At $c = 0$ the diffusion coefficient is aD_0. The function of the diffusion coefficient can be described as

$$D(c) = D_0\left[(1-a)\frac{c}{c_0} + a\right]. \tag{10}$$

Considering the dimensionless concentration c^* used in the previous model, the diffusion coefficient is

$$D(c^*) = D_0[(1-a)(c^* + 1/2) + a]. \tag{11}$$

The coefficient a in (10) and (11) describes the interaction between the molecules of the solute A and the solvent B:

- If $a = 1$, all interactions of A–A, B–B and A–B are equal, the mixing model is ideal and linear because of the constant diffusion coefficient $D = D_0$.
- If $a < 1$, the interaction A–B is stronger than A–A. Thus, it is more difficult for A to freely move in B than in A. The diffusion coefficient at low concentration of A is smaller.
- If $a > 1$, the interaction A–B is weaker than A–A. Thus, the diffusion coefficient at low concentration of A is larger.

The behavior described in (11) was observed in many binary solutions [17, 18]. With this nonlinear model, the Peclet number in (4) has the form

$$Pe(c^*) = \frac{Pe_0}{a + (1-a)c^*}, \tag{12}$$

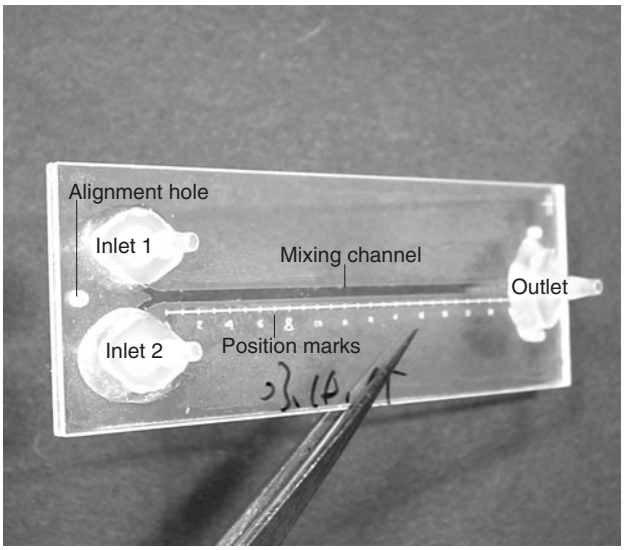

Figure 3. The polymeric device for mixing experiments.

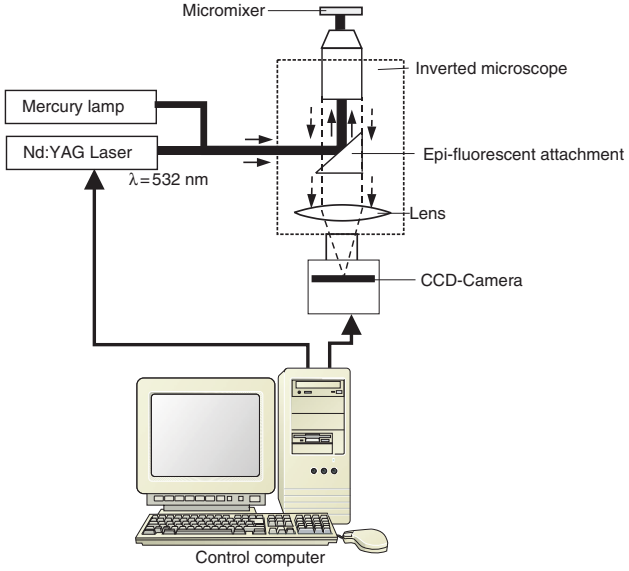

Figure 4. Experimental setup for micro-PIV measurement and mixing measurement.

where Pe_0 is the Peclet number evaluated with D_0. Equation (4) is difficult to solve explicitly with (12). However, an iteration method can be used. The calculation starts with the linear solution (7). The next iteration determines the new Peclet numbers with (12) using the concentration calculated in the previous iteration. The results often converge after just three iterations.

Figure 2 compares the results of the linear model ($a = 1$, figure 2(a) with the nonlinear models ($a < 1$, figure 2(b)) and ($a > 1$, figure 2(c)).

3. Experiments

3.1. Materials and method

Figure 3 depicts the test device used in the experiments of this paper. The 25 mm $\times$ 75 mm device is made entirely of polymer (polymethylmethacrylate, PMMA). The fabrication is based on the adhesive lamination technique. First, two PMMA plates are cut using a CO_2 laser. Alignment holes, fluidic access holes and position marks are laser-machined into the PMMA substrate. Second, a double-sided adhesive sheet (Adhesives Research Inc., Arclad 8102 transfer adhesive) is cut to form the intermediate layer with the channel structures. The adhesive layer thickness of 50 μm defines the channel's height. The three layers are positioned with the alignment holes and pressed for bonding. Using this technique a mixing channel with 850 μm width and 50 μm height was fabricated for the experiments described in the next sections.

3.2. Experimental setup

An experimental setup was used for both measurements of the velocity field and the concentration field. The setup consists of four main components: an illumination system, an optical system, a coupled charge device (CCD) camera and a control system. The control system consisting of a peripheral component interface (PCI) card, and its corresponding software, is implemented in a personal computer (PC). The PC can control and synchronize all actions related to illumination and image recording. A schematic of the setup is illustrated in figure 4.

Two different light sources were used for the two measurements. Because of the ability of precise timing and intensity control, a laser beam was used for the micro-PIV (micro particle image velocimetry) measurement. In our system, a double pulsed Q-switched (quality switched) Nd:YAG laser was used. By including a Q-switch inside the cavity the laser can work in a triggered mode. The laser has a wavelength of 532 nm and a maximum energy of 160 mJ. The two-laser-head system allows the realization of two laser pulses with a very small delay. The system can work in different modes: single exposure in one frame, double exposure in one frame, and double exposure in double frames. In our experiments, the mode of double exposures in double frames was used because of the high signal-to-noise ratios and the better quality of the cross-correlation technique. For the concentration measurement, a single mercury lamp was used for the illumination.

The optical system was a Nikon inverted microscope (Model ECLIPSE TE2000-S) with a set of epi-fluorescent attachments. There are three optical elements in a filter cube: excitation filter, dichroic mirror and emission filter. Emission filters are used in both measurements to select more specifically the emission wavelength of the sample and to remove traces of excitation light.

An interline transfer CCD camera (Sony ICX 084) was used for recording the images. The resolution of the camera is 640 pixels $\times$ 480 pixels, with 12 bits grayscale. The active area of the CCD sensor is 6.3 mm $\times$ 4.8 mm. The minimum inter-frame transfer time, and thus the fastest time delay for the two PIV images, is 300 ns. To ensure that the CCD camera is working at its optimum temperature of $-15\,^{\circ}$C, a cooling system is integrated in the CCD camera. In the mode of double

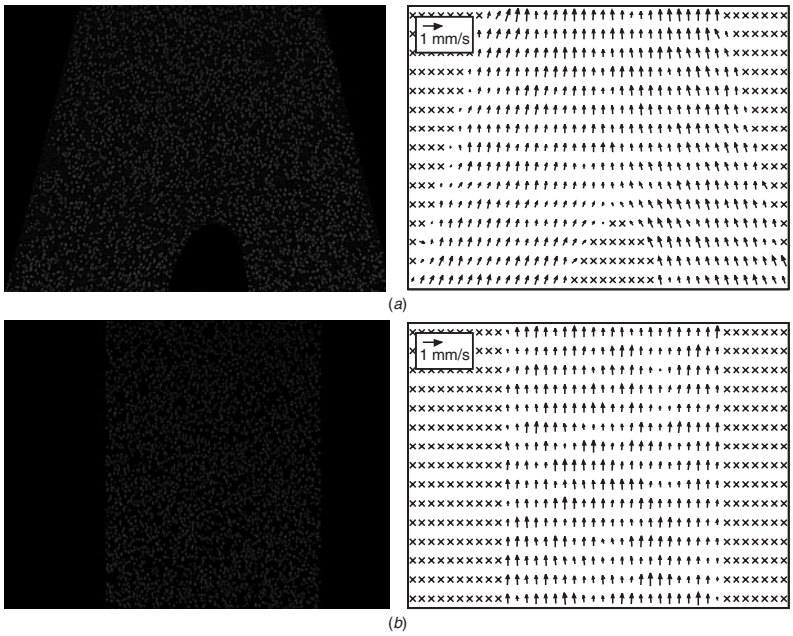

Figure 5. Results of micro-PIV measurements: (*a*) at the entrance of the mixing channel and (*b*) in the mixing channel.

exposure in double frames, the camera can record two frames of the flow fields and then digitizes them in the same image buffer.

4. Results and discussion

4.1. Micro-PIV measurement

In order to improve the signal-to-noise ratio, seeding particles with a large gap between excitation wavelength and emission wavelength were used in our experiments. We used Duke red particles (Duke Scientific Co.), which have a maximum excitation wavelength of 540 nm (green, very close to the characteristic wavelength of Nd: YAG) and a maximum emission wavelength of 610 nm (red). The diameter of the particles can be chosen from several hundreds of nanometers to several microns. The PIV-measurement uses an epi-fluorescent attachment of type Nikon G-2E/C (excitation filter for 540 nm, dichroic mirror for 565 nm and an emission filter for 605 nm). Both filters in the attachment have a bandwidth of 25 nm.

The measurement reported in this paper was carried out with a 4× objective. With a CCD sensor size of 6.3 mm × 4.8 mm, the size of an image pixel is 2.475 μm and the size of the measured area is 1584 μm × 1188 μm. Fluorescent particles with a diameter of 3 μm were used to trace the flow. The particles were diluted in deionized (DI) water, filled in two syringes, and pumped into the mixer using a syringe pump. The flow rate in the mixing channel was 200 μl h^{-1}.

Two 30 mJ laser pulses with a delay time of 3.5 ms were used as illumination sources. The integration area is 32 pixels × 32 pixels. Figure 5 shows the results of the micro-PIV measurement. The results show that the entrance length at the junction is relatively short. The velocity profile in the mixing channel is uniform. Thus, the flow in the mixing channel can be considered as a two-dimensional Hele–Shaw flow.

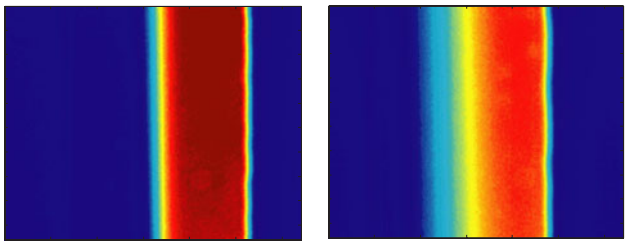

Figure 6. Intensity distribution (color coded) in the mixing channel at $u = 2$ mm s^{-1} at different positions.

4.2. Mixing measurement

For the mixing measurement, DI water was used as the solvent. The solute is a fluorescent dye (fluorescein disodium salt $C_{20}H_{10}Na_2O_5$ diluted in water). This dye is also called Acid Yellow 73 or C.I. 45350. Two identical syringes were filled with the dye solution and the DI water and placed on a syringe pump (Cole-Parmer 74900-05, 0.2 μl h^{-1} to 500 ml h^{-1}, accuracy of 0.5%). The identical syringes ensure the same flow rates for the two inlet flows.

The measured area was illuminated with a mercury lamp. For the measurement an epi-fluorescent attachment of type Nikon B-2A was used (excitation filter for 450–490 nm, dichroic mirror for 505 nm and an emission filter for 520 nm). After recording the images on the PC, the concentration profiles were evaluated using a customized program written in MATLAB. First, the program removes the noise in the measured image with an adaptive noise-removal

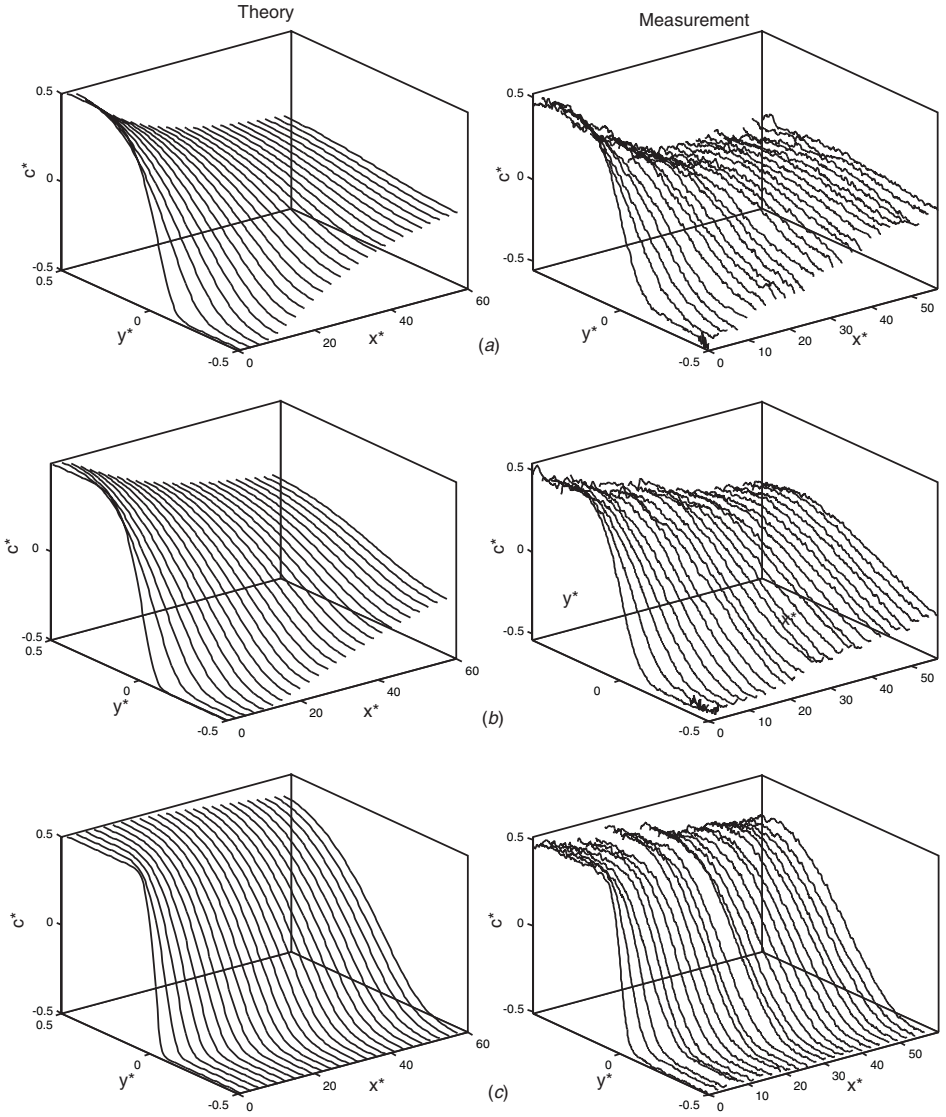

Figure 7. Dimensionless concentration distribution in the mixing channel: (*a*) $Pe_0 = 153$ ($\dot{Q} = 40\ \mu\mathrm{l\ h^{-1}}$, $u = 270\ \mu\mathrm{m\ s^{-1}}$, $Re = 18.3 \times 10^{-3}$); (*b*) $Pe_0 = 237$ ($\dot{Q} = 62\ \mu\mathrm{l\ h^{-1}}$, $u = 418\ \mu\mathrm{m\ s^{-1}}$, $Re = 28.3 \times 10^{-3}$) and (*c*) $Pe_0 = 1185$ ($\dot{Q} = 310\ \mu\mathrm{l\ h^{-1}}$, $u = 2090\ \mu\mathrm{m\ s^{-1}}$, $Re = 141.7 \times 10^{-3}$).

filter. For each pixel, a local mean value is calculated for a window of 5×5 pixels. The noise distribution is assumed to be the Gaussian distribution. Subsequently, a path with a known position across the channel is evaluated. The position across the channel is normalized against the channel width $y^* = y/W$, while the measured pixel intensity I is normalized against the maximum $I_{\max}$ and minimum $I_{\min}$ of the intensity at the inlet:

$$I^* = \frac{I - I_{\min}}{I_{\max} - I_{\min}} - \frac{1}{2}. \tag{13}$$

The measured dimensionless intensity is assumed to be equal to the dimensionless concentration of the fluorescent dye ($I^* = c^*$). Figure 6 shows the typical intensity distribution in the mixing channel.

Because of both the unknown diffusion coefficient D_0 and the factor a, the theory presented in section 2.2 was used for fitting the measurement results. While the solute side ($c^* = 1/2$) was used for finding D_0, the solvent side ($c^* = -1/2$) was used for determining the factor a. First, the model uses $a = 1$ (linear model) for finding D_0. The diffusion coefficient D_0 is found if the analytical solution matches the measurement at the solute side ($c^* = 1/2$). Subsequently, the diffusion coefficient D_0 determined in the first step was used in the model for finding a. The factor a is found if the analytical solution matches the measurement at the solvent side ($c^* = -1/2$). Using several measurements at different average velocities, the parameters $a = 0.4$ and $D_0 = 1.5 \times 10^{-9}\ \mathrm{m^2\ s^{-1}}$ were found for the experiments presented in this paper. Figure 7 compares the measurement results with the theoretical results using the above fitting parameters.

Figure 8 compares the measured concentration profiles and concentration gradient profiles with the theoretical results using the fitting parameters mentioned above. It can be seen clearly that the nonlinear model describes well the diffusive mixing process in the microchannel. The broadening band can be observed with the gradient profile. The band is thinner at a higher Peclet number.

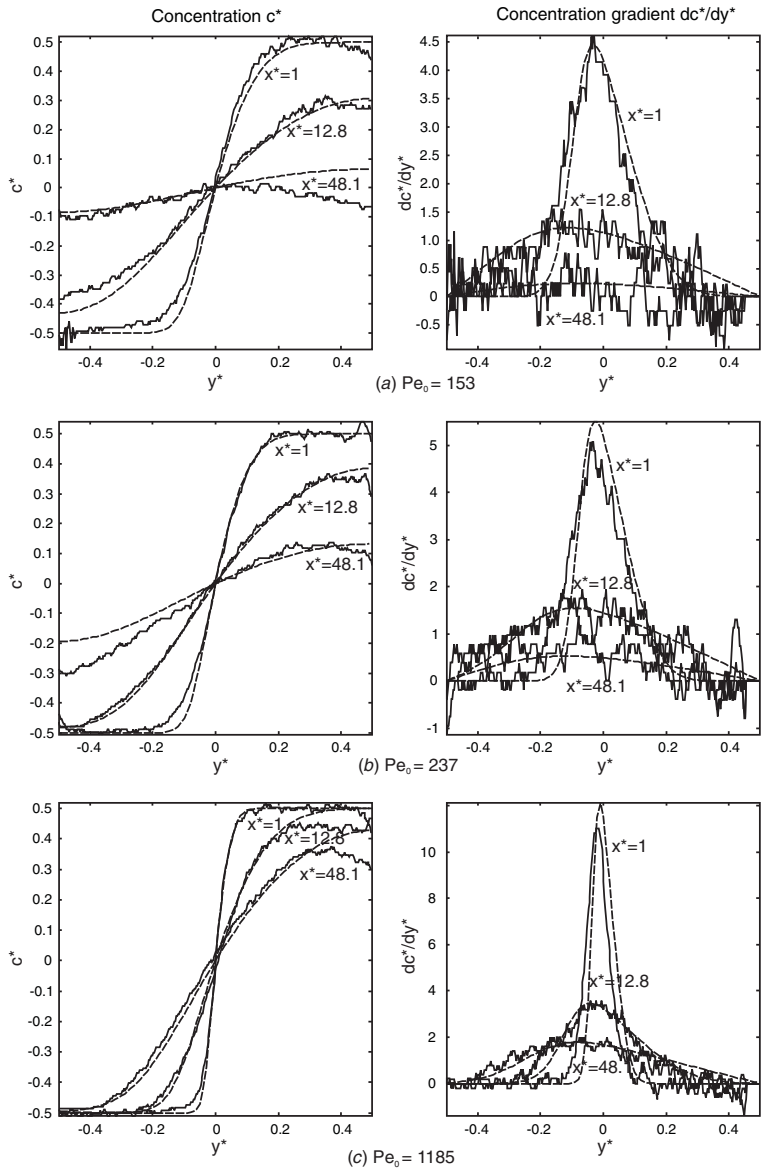

Figure 8. Distributions of concentration and concentration gradient across the mixing channel at $x^* = 1$, $x^* = 12.8$ and $x^* = 48.1$ (solid lines are measured results, dashed lines are theoretical results with $D_0 = 1.5 \times 10^{-9}$ and $a = 0.4$): (*a*) $Pe_0 = 153$; (*b*) $Pe_0 = 237$ and (*c*) $Pe_0 = 1185$.

5. Conclusions

A nonlinear model has been developed for diffusive mixing in a microchannel. The model takes into account a linear dependency of the diffusion coefficient on the concentration. The parameters describing this dependency are the diffusion coefficient at 100% concentration D_0 and the factor a for the diffusion coefficient at 0% concentration. The factor a characterizes the interaction between the solvent and the solute. The conventional linear mixing model can be described with $a = 1$. Experiments were carried out to verify this theory. A diluted fluorescent dye (Acid Yellow 73) was used as the solute. Although both a and D_0 are unknown for the solute in the experiments, the nonlinear model is well suited for fitting the experimental results. The parameters $a = 0.4$ and $D_0 = 1.5 \times 10^{-9}$ m^2 s^{-1} were determined for the test solute. A factor a less than 1 indicates that the diffusion coefficient is smaller at a lower concentration, which can be seen clearly in the measured asymmetrical concentration profile. This nonlinear model can be used for optimizing microfluidic devices related to diffusive mixing.

Acknowledgments

This work was supported by the academic research fund of the Ministry of Education Singapore, contract number RG11/02. The first author wishes to gratefully acknowledge the PhD scholarship from Nanyang Technological University.

References

[1] Nguyen N T and Wereley S T 2002 *Fundamentals and Applications of Microfluidics* (Boston: Artech House Publishers)

[2] Gobby D *et al* 2001 Mixing characteristics of T-type microfluidic mixers *J. Micromech. Microeng.* **11** 126–32
[3] Jackman R J *et al* 2001 Microfluidic systems with on-line UV detection fabricated in phorodefineable epoxy *J. Micromech. Microeng.* **11** 263–9
[4] Schwesinger N *et al* 1996 A modular microfluid system with an integrated micromixer *J. Micromech. Microeng.* **6** 99–102
[5] Gray B L *et al* 1999 Novel interconnection technologies for integrated microfluidic systems *Sensors Actuators* A **77** 57–65
[6] Miyake R *et al* 1993 Micro mixer with fast diffusion *Proc. MEMS'93, 6th IEEE Int. Workshop on Micro Electromechanical Systems* pp 248–53
[7] Evans J *et al* 1997 Planar laminar mixer *Proc. MEMS'97, 10th IEEE Int. Workshop on Micro Electromechanical Systems* pp 96–101
[8] Yang Z *et al* 2001 Ultrasonic micromixer for microfluidic systems *Sensors Actuators* A **93** 266–72
[9] Bao H H *et al* 2001 A minute magneto hydro dynamic (MHD) mixer *Sensors Actuators* B **79** 207–15
[10] Oddy M H *et al* 2001 Electrokinetic instability micromixing *Anal. Chem.* **73** 5822–32
[11] Kamholz A E *et al* 1999 Quantitative analysis of molecular interaction in microfluidic channel: the T-sensor *Anal. Chem.* **71** 5340–7
[12] Beard D A 2001 Taylor dispersion of a solute in a microfluidic channel *J. Appl. Phys.* **89** 4667–9
[13] Holden M A *et al* 2003 Generating fixed concentration arrays in a microfluidic device *Sensors Actuators* B **92** 199–207
[14] Jacobson S C *et al* 1999 Microfluidic devices for electrokinetic driven parallel and serial mixing *Anal. Chem.* **71** 4455–9
[15] Gaskell D R 1995 *Introduction to Thermodynamics of Materials* (London: Taylor and Francis)
[16] Cussler E L 1984 *Diffusion: Mass Transfer in Fluid Systems* (New York: Cambridge University Press)
[17] Bassi F A *et al* 1977 An improved optical method of obtaining the diffusion coefficient from the refractive index gradient profile *J. Phys. E: Sci. Instrum.* **10** 249–53
[18] Timmermans J 1960 *The Physio-Chemical Constants of Binary Systems in Concentrated Solution* (New York: Interscience)